Double-cladding-fiber-based detection system for intravascular mapping of fluorescent molecular probes

R. Nika Razansky[1,*], Amir Rozental[1], Mathias S. Mueller[2], Nikolaos Deliolanis[1], Farouc A. Jaffer[3], Alexander W. Koch[2] and Vasilis Ntziachristos[1]

[1]Chair for Biological Imaging, Technische Universität München, Klinikum rechts der Isar, Ismaningerstr. 22, Munich, Germany
[2]Chair for Measurement Systems and Sensor Technology of Optics, Technische Universität München, Munich, Germany D-80290
[3]Cardiovascular Research Center (CVRC) and Cardiology Division, Massachusetts General Hospital and Harvard Medical School, Boston MA, USA

ABSTRACT

Early detection of high-risk coronary atherosclerosis remains an unmet clinical challenge. We have previously demonstrated a near-infrared fluorescence catheter system for two-dimensional intravascular detection of fluorescence molecular probes [1]. In this work we improve the system performance by introducing a novel high resolution sensor. The main challenge of the intravascular sensor is to provide a highly focused spot at an application relevant distance on one hand and a highly efficient collection of emitted light on the other.

We suggest employing a double cladding optical fiber (DCF) in combination with focusing optics to provide a sensor with both highly focused excitation light and highly efficient fluorescent light collection. The excitation laser is coupled into the single mode core of DCF and guided through a focusing element and a right angle prism. The resulting side-fired beam exhibits a small spot diameter (50 μm) throughout a distance of up to 2 mm from the sensor. This is the distance of interest for intravascular coronary imaging application, determined by an average human coronary artery diameter. At the blood vessel wall, an activatable fluorescence molecular probe is excited in the diseased lesions. Next light of slightly shifted wavelength emits only in the places of the inflammations, associated with dangerous plaques [2]. The emitted light is collected by the cladding of the DCF, with a large collection angle (NA=0.4). The double-cladding acts as multimodal fiber and guides the collected light to the photo detection elements. The sensor automatically rotates and pulled-back, while each scanned point is mapped according to the amount of detected fluorescent emission. The resulting map of fluorescence activity helps to associate the atherosclerotic plaques with the inflammation process. The presented detection system is a valuable tool in the intravascular plaque detection and can help to differentiate the atherosclerotic plaques based on their biological activity, identify the ones that prone to rupture and therefore require more medical attention.

Keywords: Intravascular imaging, near-infrared fluorescence detection, molecular probe, double cladding fiber, vulnerable plaque

nika.razansky@tum.de; phone: +4917624890156; fax: +49-31873008

Optical Fibers, Sensors, and Devices for Biomedical Diagnostics and Treatment XI, edited by Israel Gannot, Proc. of SPIE Vol. 7894, 78940K · © 2011 SPIE · CCC code: 1605-7422/11/$18 · doi: 10.1117/12.874653

INTRODUCTION

Myocardial infarction due to atherosclerotic plaque rupture is a leading cause of morbidity and mortality worldwide. The earliest possible detection of inflammation-related plaque instability and the overall accurate characterization of coronary atherosclerosis remains the holy grail for the prevention of myocardial infarction. It requires sensitive molecular imaging techniques in combination with currently existing morphological imaging modalities.

Numerous scientific groups focus on development of imaging techniques that are capable to identify vulnerable plaques before rapture. A number of diagnostic modalities are available in clinical practice today, and others are going through different stages of development and preclinical trials [4].

Cardiovascular imaging modalities are divided into two basic categories: non-invasive and invasive imaging techniques. Main non-invasive imaging techniques include: computer tomography (CT), magnetic resonance imaging (MRI) and positron emission tomography (PET).

Despite of obvious advantages, like easy implementation and less potential complication for the patients, non-invasive modalities cannot provide appropriate solution due to their current status, i.e. insufficient resolution and sensitivity of detection, respiratory artifacts and side effects like ionizing radiation. Therefore the need for invasive coronary imaging modalities is obvious.

Several intravascular imaging techniques have been developed for direct visualization of the blood vessel wall, utilizing an intravascular catheter system. Underlying imaging technologies are different for available modalities and include reflected ultrasound waves (Intravascular Ultrasounds-IVUS) and derived modalities [5-9], optical interferometery (Optical coherence tomography- OCT) and derived modalities [10], spectral detection of chemical composition of the plaque (Raman spectroscopy, Nearinfrared time-resolved spectroscopy) [12-13] or internal lumen visualization by the means of coronary angioscopy [11]. The basic imaging process requires insertion of the catheter through the groin vein, followed by introduction into coronary arteries. The positioning is carefully monitored by the means of angiogram. Once the catheter is at the place of interest, the intravascular imaging performed and catheter is removed. Therefore, the whole procedure usually performed ambulatory takes no longer then 15 minutes, while the patient is locally anesthetized.

Detailed review of currently available intravascular imaging modalities was updated recently [2].

Visualization of cellular and molecular biomarkers is an emerging field in intravascular imaging and could offer significant complementary or surrogate information to the current clinical imaging mainstream. In vivo detection of these markers is expected to significantly improve the accuracy of predicting disease progression and to lead to efficient, patient-tailored treatments. Several solutions (e.g. 18F-fluorodeoxyglucose enhanced PET, ultrasmall superparamagnetic iron oxide enhanced MRI) have demonstrated clinical potential for molecular imaging of inflammation in large arteries, such as the aorta, carotid, and iliac arteries.

While morphology and spectral vessel composition reveal important information of atheroma progression, key cellular, biochemical and molecular mediators of the disease can further provide useful biomarkers associated with plaque instability.

Recently the detection of the fluorescence activatable probes, sensitive to inflammation proteases was found to be feasible in the plaque evaluation. These are fluorochromes that are dark in their native state and fluorescent only upon interaction with specific proteases, inflammation in this case. Those fluorochromes absorb and emit in the NIR imaging window, avoiding limitations common to both visible and infrared light, due to biological absorbers, hemoglobin in the visible light and water/lipids in the infrared.

Detection of NIR fluorescence (NIRF) from hollow organs, such as vessels, has been reported previously by our group [1,14,15]. The detection was done by a one-dimensional, fiber optic based, intravascular wire system for molecular fluorescence sensing of atherosclerosis. The flexible, narrow diameter NIRF catheter that permits in vivo, intravascular NIRF sensing was introduced. The ability of the

NIRF catheter to visualize inflammatory protease activity in real-time in vivo in rabbit atheroma, along with the effects of blood absorption on the NIRF signal, and the association between NIRF signals and histological measures of inflammation were investigated.

While this one-dimensional manual pullback system has showcased the feasibility of detecting fluorescence in vivo in animal models, it did not generate anatomically accurate vessel images and it is overall not appropriate for clinical intervention. Since 2008, we have also developed a stand-alone two-dimensional imaging system, as it will be described in preliminary studies [2]. This 2D NIRF catheter system allows blood vessel surface fluorescence mapping in real-time in vivo. However, it had several serious limitations: (i) poor spatial resolution, compared to other intravascular imaging modalities; (ii) registration with anatomical imaging modality to describe plaque biological activity was lacking; (iii) only blood vessel surface fluorescence activity was mapped, but not depth resolution of the fluorescence distribution as common to IVUS or OCT.

In order to improve the detected resolution and sensitivity we further improve the 2D NIRF setup by employing double cladding optical fiber (DCF) instead of multimodal one. DCF has been demonstrated previously in endoscopy, OCT combined fluorescence and fluorescence measurements. In this work we introduce the principle of operation in the intravascular detection and schematics of the new system along with basic performance capabilities.

METHODS

The proposed detection system utilizes DCF capability to guide single mode light in the core (typical diameter 5μm and NA=0.16) and multimodal light in the cladding (cladding diameter 125μm and NA=0.46). Below is a schematics and brief description of the apparatus:

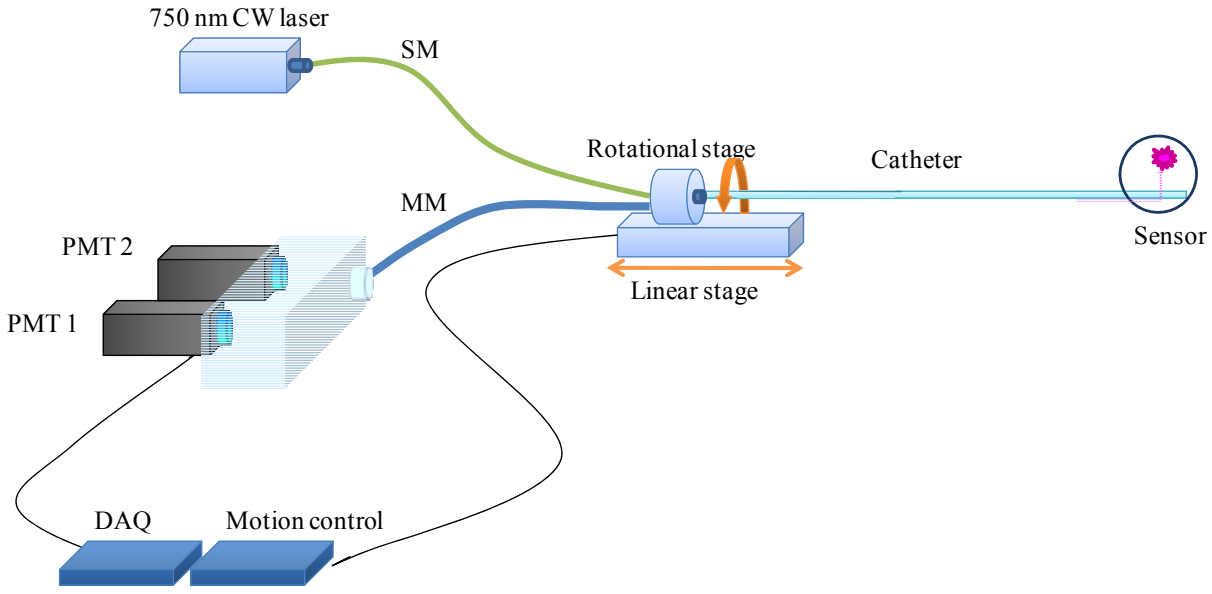

Fig.1 NIRF detection system based on the DCF schematics.

The excitation laser, coupled into single mode fiber (SM), then is filtered by fiber based filter, and coupled into DCF with the coupler. The fiber is connected to the rotational coupler and is part of the pull back device, while the front end, inside the catheter, introduced into region of interest and contains the sensor tip. The collected light is guided back by the DCF cladding to the coupler and coupled into multimodal fiber (MM) and detected by the photodetectors (PMT-photo-multiplying tube in this case). The detected signal is separated by diachroic mirror to detect fluorescence and intrinsic spectrum (PMT1 and PMT2) for subsequent signal analysis. Then the signal is digitized and recorded. Following processing step, the fluorescence signal is mapped into 2D activity of the vessel internal surface.
The previous system design was updated to incorporate DCF efficiently. Additional effort was invested into sensor tip design (Fig.2). Sensor tip is equipped with GRIN lens and right angle prism or 45^{o} mirror coating that result in side firing beam with low diverging angle. The sensor tip is crucial part of the setup, since it has to provide on one hand low diverging, small diameter excitation spot, that results in increased detection resolution. On the other hand the senor has to provide efficient emission collection. Due to high NA of the cladding (about 0.41) high portion of emission light is being collected. We suggest employing GRIN lens and right angle prism in order to optimize sensor excitation/ detection performance.

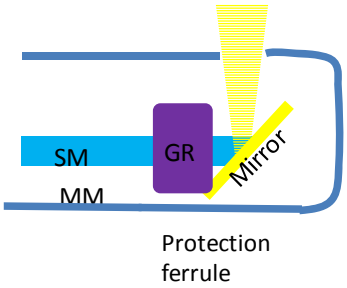

Fig.2 DCF based sensor schematics.

In this work we describe initial prove of principle of the proposed sensor design, where the double cladding fiber performance in the near-infrared spectrum is the bottle neck of this project. We had first to verify basic DCF ability to guide light in the near-infrared spectrum. Then we had studied the absorption of the light by the fiber cladding. When we were convinced that the fiber is feasible to guide mear-infrared light, we have proceeded with further fiber specs evaluation. We have measured with simple CCD camera both exciting and collection spot size and determine FWHM for both single mode and multimode cladding guided light. These are important parameters that have to be taken into account when designing the front end optics. Then we have established GRIN side firing assembly (Fig.2) and have managed to create experimental set up that can exhibit tightly focused low diverging beam up to 2 mm distance from the fiber.

RESULTS

Current detection system based on unique features of the DCF and therefore we first need to prove feasibility of DCF in this sort of measurements. We have focused our effort on the passive double cladding fiber (nLight Corporation, Lohje, Finland) that has technical specs compatible to our task. The passive fiber has no additional doping material compared to active, so we can expect less autofluorescence signal in the near-infrared spectrum.

First we have measured fiber ability to guide the light in the near-infrared spectrum and the cladding absorption of the light as a function of fiber length (Fig.3). Since the DCF was not designed for the near-infrared wavelengths, we could not rely on the absorption factor from technical specifications provided by vendor.

Results are presented in the Fig.3 below. We have measured 3 different fiber lengths (1m, 1.55m and 2m) where different laser power was coupled each time. The X-axis presents the laser power control current in amperes applied at each measurement, where Y-axis is the peak intensity detected by the CCD camera and further processed by Matlab (Mathwork Inc, Natick, MA, USA). For each of three measured lengths fiber was realigned and coupling was optimized. Generally all three obtained curves correlate with expected laser power behavior as a function of applied current. In case of ideally repeated conditions one would expect 3 parallel curves, however, due to realignment each time, the conditions were not identically preserved and, as a result the curves are slightly shifted. Therefore we have concluded that the differences in the curves' shapes are due to realignment and measurement errors and not to different lengths absorption. The absorption factor is then below our detection measurement error and therefore we can proceed and utilize this fiber in the near-infrared spectrum.

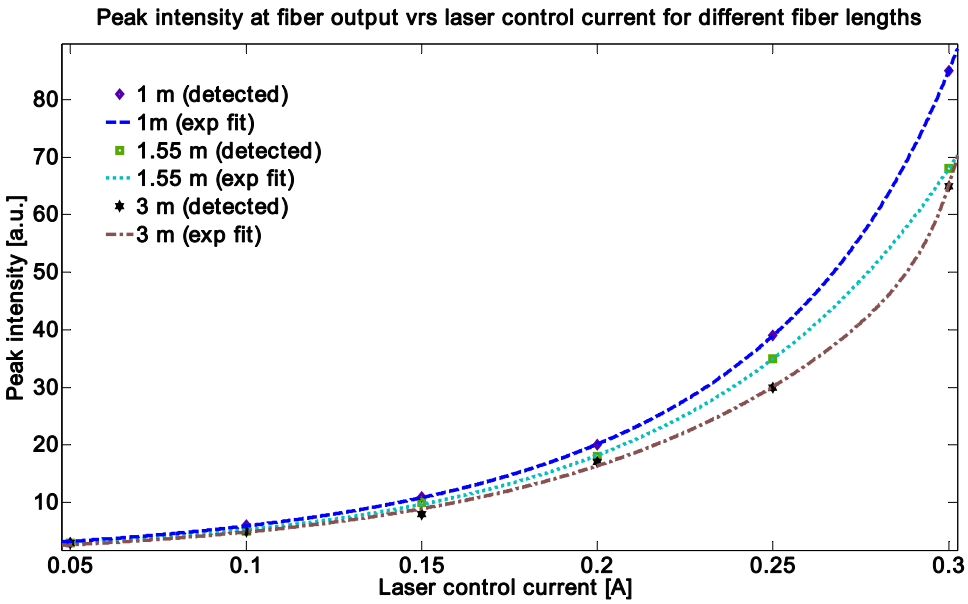

Fig. 3 Peak intensity measured at the fiber output as a function of coupled laser power for different fiber lengths.

Next, in order to determine single mode core numerical aperture, that eventually determines engineering parameters for the sensor optics, we have coupled the light into single mode core and collected near field image of the beam with CCD camera. We have applied mode stripping technique, by removing the coating and bending fiber, so we end up measuring only core guided single mode light. Then FWHM beam diameter of the detected single mode light was calculated.

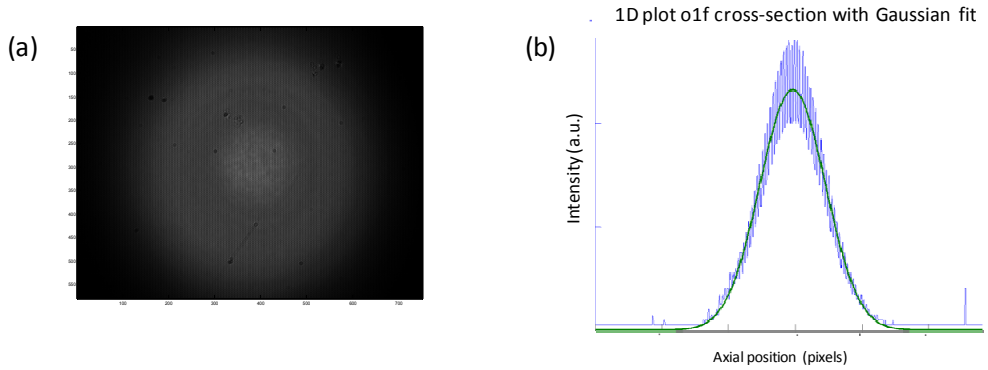

Fig. 4 (a) double cladding fiber double ring, (b) intensity plot for the single mode excitation and Gaussian fit

Fig.4 (a) showcased double cladding fiber characteristic two concentric rings detected before mode stripping, where Fig. 4(b) presents 1D plot of the single mode light detected after mode stripping. The detected images are converted to 1D intensity plot and Gaussian fit is applied using Matlab. Based on the Gaussian fit FWHM of the curve was then calculated and recorded as a spot diameter at given distance from the fiber. Detected spot size for both single mode from the core and multimodal light from the cladding corresponds to the provided NA values on the specs of the fiber; therefore justify the subsequent utilization of the fiber for Near-infrared spectrum measurements and sensor design.
Once the DCF was approved for the apparatus design we have concentrated on the sensor tip assembly. From mechanical stand point the cladding has to be stripped to allow light to propagate and to be collected by the DCF, on the other hand the light collected by the cladding has to be guided back to the detection, therefore it is crucial to preserve cladding/coating refractive index ratio. To resolve this issue we suggest strip the cladding for few millimeters at the tip of the fiber and fix it inside ferrule with limited window to exit. The fiber will be fixed inside of the ferrule with matched refractive index epoxy to keep the coating/ cladding refractive index ration. (Fig.2)
From optical stand point we need to design sensor tip that will deliver narrow spot size for the region of interest while collect as much of the spatially incoherent radiation originating as fluorescent light from the measurement site. The core of the DCF is used to illumination while cladding acts as multimodal fiber to collect the light using cladding / coating guidance.
The beam profile will evolve similar to a Gaussian beam with a waist equal to the fundamental mode diameter 16μm [16-17]. Without any additional technical means this leads to an unwanted broad evolution of the spot size.

The intensity distribution in the emitted light region may be computed depending on the distance to the fiber tip from the Gaussian beam formulas (Eq.1, Eq.2):

$$I(r,z) = I_0 \left(\frac{w_0}{w(z)} \right)^2 e^{-\frac{2r^2}{w^2(z)}} \qquad (1)$$

$$w(z) = w_0 \sqrt{1 + \left(\frac{\lambda z}{\pi w_0^2} \right)^2} \qquad (2)$$

With a mode field diameter of approximately 8 μm, the width of the beam at the position of the object (2 mm) is 254 μm, which is above the intended spot size of approximately 30 μm. When leaving the (transparent) fiber coating the beam has a diameter of 18 μm. A theoretically optimal beam shape that is achievable with Gaussian beams is shown in Fig. . The beam diameter is approximately 40 μm at the focus.

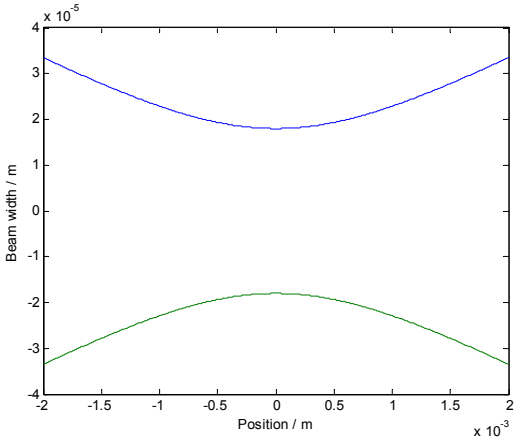

Fig. 5: Evolution of beam diameter for a beam waist of 18 µm and a beam length of +- 2 mm.

To shape the Gaussian beam into a form which is optimally suited for the application, meaning a narrow beam over a length of several millimeters, the light from the single mode fiber is conventionally guided through a GRIN medium, typically made from a piece of graded index fiber. After the single mode fiber, a piece of GRIN fiber, with appropriate length is positioned. To have an additional degree of freedom, the GRIN fiber is separated from the single mode fiber by a certain distance.

To be able to easily change the length of the GRIN fiber part and to vary the distance between single mode fiber and GRIN fiber, a glass capillary is employed. The capillary has an inner diameter of 127 µm, such that the optical fiber with an outer diameter of 125 µm tightly fit inside. This also ensures the optical alignment of the components. When varying the distance between single mode fiber and GRIN fiber, an air gap is created, that may lead to interference and stray light, distracting the characterization of the sensor tip. We therefore fill the gap between the two fibers with index matching oil, with a refractive index of 1.46, which is approximately that of the fibers.

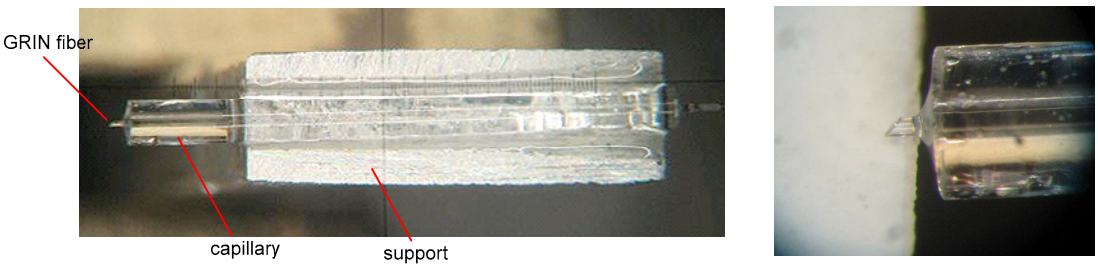

Fig. 6 Photo of the sensor (a) Image of capillary with GRIN fiber and single mode fiber connected by index matching fluid, (b) close up of angle polished fiber in capillary.

Fig.6 (a) shows the capillary mounted on a support structure for alignment with the detection optics. The capillary is 15 mm long. At the left end of the capillary, the GRIN fiber is visible, with a 450 degree angle polished end. On the right hand side of the capillary, the single mode fiber guiding the laser light is visible.

The 45° angle polish of the GRIN fiber is shown in a close up taken by a microscope in Fig.6b. For the polishing process, commercial polishing paper for fiber connectors is used, which is fixed on a rotating dish with adjustable angle.

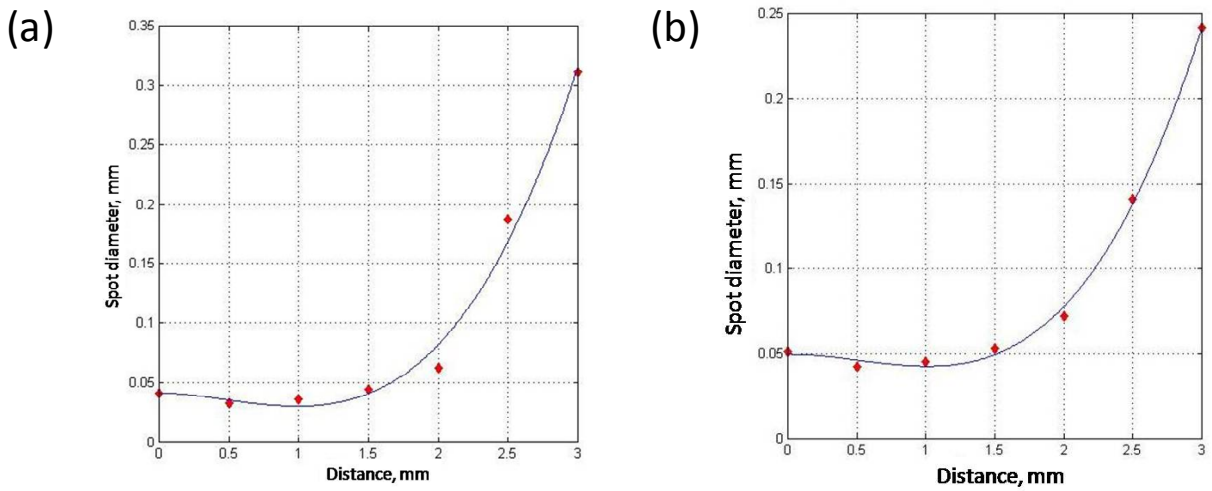

Fig. 7 Spot size vs. distance from the fiber tip at 1800 polished fiber (a) and 450 polished fiber (b) . The experimental results fit well with theoretical spot size, predicted (Fig. 4).

The excitation spot size, produced by the sensor was captured by a simple CCD camera at different distances from the sensor tip. The recorded images were processed and the FWHM spot size diameter was calculated, assuming a Gaussian beam distribution. First, the 180^0 polished GRIN lens spot size was measured in front of the fiber tip. The results are plotted in the Fig. 7. The data fits well to the theoretically predicted spot diameter of about 40 μm at the focusing point (Fig. 5).

Next the spot size was measured at the 45^0 side firing fiber. The beam spot was recorded and processed in the same way as in the previous experiment. The spot diameter versus distance from the fiber tip is plotted in Fig. 7(b). The measured spot size is quite similar to the measured spot size at 180^0 and correlates very well with the theoretical beam diameter. These results suggest an optimal distance between the GRIN lens and SM fiber in combination with the optimal GRIN lens length achieved in the current experimental design.

CONCLUSIONS

In order to improve existing NIRF detection we have introduced DCF sensor. We have demonstrated DCF advantages and feasibility for NIRF imaging. Based on DCF new detection sensor was introduced.

The new sensor requires technical update of the automatic detection system, while providing several dramatic improvements in the detection system technical performance. The excitation resolution was shown to improve in a factor of 6, compared to the first generation NIRF system, while optimized fluorescence detection ability is preserved. Therefore the spatial resolution and sensitivity of the updated system will also improve. In addition the low diverging tightly focused beam minimizes resolution dependence on the catheter distance from the blood vessel wall. This feature is crucial for minimizing artifacts and improving detection accuracy in the pre-clinical in vivo studies.

We have demonstrated the feasibility of the DCF for fluorescence probe detection. The technical specs of the demonstrated sensor allow increased detection resolution and sensitivity. At the same time the new design will further improve intravascular detection accuracy. The low diverging tight excitation spot will

allow accurately detect inflamed plaque regardless of the catheter position relatively to the blood vessel wall.

The current study demonstrates an experimental design and the manufacturing of the sensor head, while our main goal is to have a fully functioning high resolution detection system that aims towards clinical application. In order to progress towards this goal we intend to incorporate the sensor into the existing NIRF detection system3 and perform sets of system characterization studies, followed by atherosclerosis detection in in-vivo measurements.

As the next step we will perform short pilot in vivo study to prove the capability of the DCF based NIRF detection in vivo through blood. The acquired image is then will be registered with the anatomical modality (IVUS or OCT) based on the angiogram registration of the catheter tip.

The importance of vulnerable plaques early detection cannot be overestimated 18, therefore our system is tailored towards pre-clinical implementation and in-vivo trials, to allow rapid 'benchside – bedside' translation.

REFERENCES

[1] Chang K, Jaffer F. J, "Advances in fluorescence imaging of the cardiovascular system," Nucl Cardiol 15, 417-28 (2009)

[2] W. A. Reed, M.F. Yan, M. J. Schnitzer,"Gradient-index fiber-optic microprobes for minimally invasive in vivo low-coherence interferometry," Optics Letters 27(20), 1794-1796 (2002)

[3] Razanksy R.N., Rosenthal A., Mallas G., Razansky D., Jaffer F.A., Ntziachristos V., "Near-infrared fluorescence intravascular catheter system for two-dimensional intravascular imaging in vivo", Optics Express

[4] Schaar JA, Mastik F, Regar E, den Uil CA, Gijsen FJ, et al.," Current diagnostic modalities for vulnerable plaque detection", Current Pharmaceutical Design 13, 995-1001 (2007)

[5] Nissen S, Yock P. "Intravascular ultrasound: novel pathophysiological insights and current clinical applications", Circulation 103,604-16 (2001)

[6] Nair A, Kuban B, Tuzcu E, Schoenhagen P, Nissen S, Vince D. "Coronary plaque classification with intravascular ultrasound radiofrequency data analysis", Circulation 106, 2200-6 (2002)

[7] Granada J, Wallace-Bradley D, Win H, Alviar C, Builes A, et al. " In vivo plaque characterization using intravascular ultrasound-virtual histology in a porcine model of complex coronary lesions", Arterioscler Thromb Vasc Biol 27, 387-93 (2007)

[8] de Korte C, Pasterkamp G, van der Steen A, Woutman H, Bom N. "Characterization of plaque components with intravascular ultrasound elastography in human femoral and coronary arteries in vitro", Circulation 102,617-23 (2000)

[9] Schaar J, de Korte C, Mastik F, Baldewsing R, Regar E, et al. " Intravascular palpography for high-risk vulnerable plaque assessment", Herz 28,488-95 (2003)

[10] Stamper D, Weissman N, Brezinski M. 2006. " Plaque characterization with optical coherence tomography", J Am Coll Cardiol 47C, 69-79 (2006)

[11] White C, Ramee S, Collins T, Murgo J., " Coronary angioscopy", Tex Heart Inst J 22,20-5 (1995)

[12] Brennan JF, Nazemi J, Motz J, Ramcharitar S." The vPredict Optical Catheter System: Intravascular Raman Spectroscopy", EuroIntervention 3, 635-8 (2008)

[13] Gardner, C.; Tan, H.; Hull, E.; Lisauskas, J.; Sum, S.; Meese, T.; Jiang, C.; Madden, S.; Caplan, J.; Burke, A.; Virmani, R.; Goldstein, J.; Muller, J.," Detection of lipid core coronary plaques in autopsy specimens with a novel catheter-based near-infrared spectroscopy system." JACC Cardiovasc Imaging, *1* (5), 638-48 (2008)

[14] Zhu B, Jaffer F, Ntziachristos V, Weissleder R." Development of a near infrared fluorescence catheter: operating characteristics and feasibility for atherosclerotic plaque detection", Journal of Physics, D-Applied Physics 38,2701-7 (2005)

[15] Jaffer FA, Vinegoni C, John MC, Aikawa E, Gold HK, et al." Real-time catheter molecular sensing of inflammation in proteolytically active atherosclerosis", Circulation 118,1802-9 (2008)

[16] Li X, Chudoba C, Ko T, Pitris C, Fujimoto J." Imaging needle for optical coherence tomography", Optics Letters 25,1520-2 (2000)

[17] Fujimoto JG. , "Optical coherence tomography for ultrahigh resolution in vivo imaging", Nature Biotechnology 21,1361-7 (2003)